

# Comparative Study on Gamma Radiation Attenuation Parameters between In-House Developed and Locally Available Shielding Materials

ROSHLAN RAHMAN DIPTO, ABDUS SATTAR MOLLAH  
Department of Nuclear Science and Engineering  
Military Institute of Science and Technology  
Dhaka, BANGLADESH

*Abstract:* - This study presents calculation of gamma attenuation parameters for in-house developed Polyboron and Borated polyethylene shielding materials and locally available shielding materials like Pure polyethylene, water and ordinary concrete which can be used as potential radiation shielding materials. The study was carried out using GEANT4 which is a software arrangement, a combination of tools which can be used to simulate the particle transportation accurately through matter. The results were compared and in good match have been observed with the database of XCOM taking photon energy range 40 keV-20 MeV. For each energy 10000 particles were transported through the slab. Relaxation-lengths have been also calculated from obtaining linear attenuation coefficients. The obtained result shows Mass attenuation coefficient, Linear attenuation coefficient and relaxation length density of the shielding materials on the photon energy. The total Mass attenuation coefficient ( $\mu_m$ ), Linear attenuation coefficient ( $\mu$ ), Half Value Layer (HVL) and Tenth Value Layer (TVL) of each material for some mostly used gamma radiation sources has been calculated. The study's findings can be used to understand how effective shielding is in reactor shielding, containment buildings, nuclear spent fuel casks and other shielding scenarios. These materials are engineered solutions intended to maximize safety, utility, and cost-effectiveness in radiation situations; they are more than merely barriers. As radiation technologies advance, it is crucial that they be continuously studied, optimized, and combined.

*Key-Words:* - Radiation; GEANT4; Polyboron; Reactor; Nuclear spent fuel cask; Gamma

Received: April 16, 2024. Revised: March 9, 2025. Accepted: April 4, 2025. Published: May 26, 2025.

## 1 Introduction

Use of Nuclear technology with time in research, agriculture, health sector and nuclear energy production are increasing day after day. One of the main concerns of dealing with nuclear technology is the radiation which can be exposed to the outside environment and human beings and it can cause severe incidents. So, the radiation must be absorbed enough so that the personnel can be protected from the effects caused by radiation [1]. In reactor environments, industry, and nuclear medicine, gamma radiation shielding is essential. Conventional materials including water, concrete, and lead are frequently utilized. However, other shielding materials have drawn interest because of health, economic, and environmental issues. For designing and choosing an appropriate material for shielding, it is essential to study the

characteristics of materials that are exposed to radiation. The parameters related to radiation shielding which are studied in case of designing a shield are total mass and linear attenuation coefficient, for gamma rays and these have relation with Half Value Layer (HVL), Tenth Value Layer (TVL), and Relaxation length. Researchers determine the values of different shielding parameters in different ways. The mass attenuation coefficient (mm) for polyboron, a locally produced shielding material, was analytically determined and results are compared using the WinXCom code, a Windows version of the XCOM database, at photon energies between 0.001 MeV and 20 MeV [2]. The photon attenuation coefficients of barite and barite-based concrete. For 1 keV–1 GeV energy, the linear attenuation coefficients were computed and compared with measurements made with a gamma spectrometer built with an MCA at 662,

1173, and 1332 keV and a NaI(Tl) detector [3]. In another study, Effective Atomic and Electron numbers of Stainless Steel and Mass attenuation coefficients were determined [3]. Twelve concrete samples, both with and without mineral ingredients, have been examined for their ability to shield against gamma and neutron radiation. At photon energies of 59.5 and 661 keV, measurements and calculations have been made of the atomic cross-sections, effective atomic numbers, linear and total mass attenuation coefficients, half-value thicknesses, and effective electron densities [4],[5], [6]. It is known that hydrogen rich materials are used to shield the neutron radiation to do moderation. When boron is added to these hydrogenous materials it reduces secondary gamma radiation. Some of the shielding properties of this locally developed material have been studied theoretically and experimentally [5]. The cross section of concrete, including marble, was examined for photon interaction, energy absorption, and neutron removal [7], [8]. The gamma-ray shielding properties of polyboron and ilmenite-magnetite (I-M) concrete were measured using a NaI (Tl) detector [9]. For various photon energies ranging from 1 keV to 20 MeV, the effective atomic number, effective electron density, total atomic cross-section, and total electronic cross-section of locally produced ilmenite-magnetite (I-M) concrete have been calculated analytically and compared with concretes of various densities and compositions [9]. Optimizing innovative radiation shielding materials requires the use of multi-scale models in conjunction with experimental validation, as highlighted in recent papers in WSEAS journals [10], [11]. Furthermore, several authors [12], [13] have used the Finite Element Method (FEM) to perform shielding properties for a number of shielding materials. They identified certain FEM limitations.

According to a review of the literature, the evaluation techniques usually involve the use of experimental setups, MCNP/GEANT4 simulations, or XCOM/NIST databases to determine the linear attenuation coefficient ( $\mu$ ), mass attenuation coefficient ( $\mu/\rho$ ), half-value layer (HVL), tenth-value layer (TVL), and

effective atomic number ( $Z_{eff}$ ). Despite advancements, there are still significant gaps in the comparative benchmarking of locally accessible shielding materials versus internally created composites under the same gamma source conditions. Our work advances existing frameworks by introducing material-specific elemental compositions, producing attenuation predictions that are more accurate than those obtained using previous bulk-average techniques. The main objectives of the present study are to determine the values of parameters using Geant4 simulation software and validate its viability and also to demonstrate a comparison of shielding effectiveness of the locally available and developed materials which have been used in the present work and at different photon energies.

## 2 Theoretical Background

### 2.1 Calculation of Mass and Linear Attenuation Coefficient

While traversing an absorber, the gamma ray intensity will be attenuated. This phenomenon follows the Beer-Lambert's law [14]:

$$I = I_0 e^{-\mu x} \quad \dots \quad (1)$$

Here  $I_0$  and  $I$  are intensity of gamma ray before shielded and after being shielded respectively,  $\mu$  signifies the linear attenuation coefficient of unit  $cm^{-1}$  and  $x$  means linear thickness. Mass attenuation coefficient ( $\mu_m$ ) is defined as [14],

$$\mu_m = \mu/\rho \quad \dots \quad (2)$$

$\rho$  is the material's density.

### 2.2 Calculation of TVL, HVL and Relaxation length ( $\lambda$ )

Half Value Layer (HVL) is the thickness of a shielding material or a shield for which the radiation intensity gets reduced by a factor of 2 after attenuation. This term is deliberated through the following equation:

$$\text{HVL} = \ln 2 / \mu \quad \dots \quad (3)$$

The Tenth Value Layer (TVL) is denoted the thickness for which a radiation gets decreased to 10% of its radiation level after attenuation. It is calculated by,

$$\text{TVL} = \ln 10 / \mu \quad \dots \quad (4)$$

Relaxation length ( $\lambda$ ) is defined as the mean displacement between two successive collisions or interactions. This length is defined by the equation,

$$\lambda = \frac{\int_0^{\infty} x e^{-x} dx}{\int_0^{\infty} e^{-x} dx} = \frac{1}{\mu} \quad \dots \quad (5)$$

### 3 Materials and Models

The total mass attenuation coefficient for five shielding materials –

- Ordinary Concrete
- Polyboron
- Pure polyethylene
- Borated polyethylene
- Water

has been analytically calculated using Eqs, (1-2) at gamma energy range of 40 keV to 20MeV. The calculation of the mass attenuation coefficients of these five samples has been done by Geant4 for the mentioned energy range. The analytical results obtained from the Geant4 calculation were compared with X-com values. The TVL, HVL, Linear and mass attenuation coefficient have been calculated for the same gamma radiation sources. Table 2 represents the properties of the shielding material.

#### 3.1 Geometry

The present study involves the Geant4 model for radiation shielding materials that are locally developed and available materials. A cylindrical source has been used in the model to produce radiation as needed. A typical geometry generated by the GEANT4 software is shown in Figure 1,

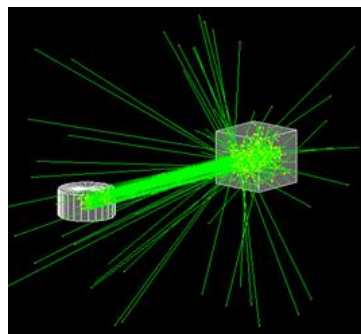


Figure 1: Geometry arrangement for simulation.

A cube shaped NaI detector has been used to detect the gamma photons radiated from the source. A slab shaped shield has been used.

#### 3.2 Simulation Software

The software that has been used in this study is “Geant4”. Geant4 which means “Geometry and Tracking” is a toolkit for the simulation of the transport of particles through material using Monte Carlo methods. It employs the principles of object-oriented programming through the use of C++. It provides its user a set of functions including tracking of particles, different types of sensitive detectors, physics models etc. [15].

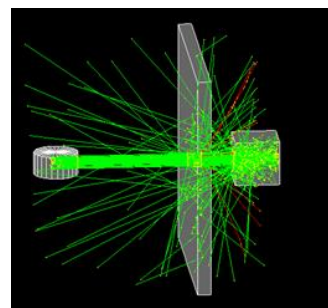


Figure 2: Gamma-ray production and interaction process in the GEANT4 software.

### 4 Set up and Methodology

In the present work, a source with a NaI detector was modelled with Geant4 [16]. In between the source and NaI, a slab of shielding material was put. To calculate the mass attenuation coefficient first gamma radiation of certain energy was emitted without any shielding material to be attenuated and the radiation was detected through the NaI detector thus calculated the absorbed dose ( $I_0$ ). Figure 1 presents a visual representation of this process. After calculating

the absorbed dose without any slab, a shielding slab with desired material was placed between the source and detector whose mass attenuation co-efficient is being calculated and the same process was done for calculating the absorbed dose (I) in the detector. Figure 2 demonstrates the gamma-ray production and attenuation process. Then, Using Equation (1) mass attenuation coefficient was calculated and serially other properties were calculated too. Typical material definition in C++ for GEANT4 code with Physics list is given below:

```
G4Element* eH = new G4Element("Hydrogen", "H", 1.,
1.01*g/mole);
G4Element* eC = new G4Element("Carbon", "C", 6.,
12.01*g/mole);
G4Material* polyethylene = new
G4Material("Polyethylene", 0.94*g/cm3, 2);
polyethylene->AddElement(eC, 0.857);
polyethylene->AddElement(eH, 0.143);

G4EmStandardPhysics* emPhysicsList = new
G4EmStandardPhysics();
runManager->SetUserInitialization(emPhysicsList);
```

## 5. Physical explanation

The interaction of photons of matter can be of four types. i) Rayleigh/Coherent scattering ii) Compton scattering iii) Photoelectric effect and iv) Pair production. For photons with low energy levels, the photoelectric effect is dominant. A study of the different theoretical methods and approximations has been given by Pratt [17] and relation between the results of some of the methods has been discussed by Gavrila [18]. For K-shell cross section, values of the high energy limit was obtained by Pratt for all values of  $\alpha Z$  through a modified plane wave approximation which is a numerical method. Analytically an equation was obtained which includes the first three terms of the power series in  $\alpha Z$ . High energy  $Z$ -dependent equation was obtained by Pratt with Gavrila's results on the energy dependence he obtains the equation stated below for the K-shell cross section:

$$a^{\tau}k = a^{\tau_0}k \frac{\beta^3}{(1-\beta^2)^{\frac{3}{2}}} \left(\frac{mc^2}{hv}\right)^4 (aZ)^{2\xi'} M(\beta) e^{[-2(\frac{\alpha Z}{\beta}) \arccos(\alpha Z)] \{1 + \pi \alpha [\frac{N(\beta)}{M(\beta)}] + R(aZ)\}} \dots \dots (6)$$

Where,

$a^{\tau_0}k$  in the sauter's equation is the high energy limit.

$\xi' = \left[(1 - \alpha^2 z^2)^{\frac{1}{2}} - 1\right] \approx \frac{-1}{2} \alpha^2 Z^2$  presents the binding energy, in  $mc^2$  units. In this interaction a single electron from an atom on absorption of the photon gets ejected out from the atom. Below 100 keV photon energy the photo electric effect dominates absorption and it is characterised by the existence of the K,L,M... absorption edges. For each K shell electron the contribution to the cross action is given by Gavrila-Pratt equation,

$$\sigma = \frac{4\pi e^4}{m^2 c^4} Z^5 \alpha^4 \left(\frac{mc^2}{hv}\right)^n \dots \dots (7)$$

$h\nu$  is the photon energy and  $n=7/2$  at  $h\nu$  (photon energy)  $< mc^2$  and changes to 1 at  $h\nu \gg mc^2$ . Equation (7) clearly shows the  $Z$  dependency of photo electric effect. Higher the  $Z$ , higher the probability of interaction of photon with matter. When  $mc^2 = h\nu$ , photo-electric peak is found. On the other hand, If the cross section of Compton scattering for per electron for the number of photons is denoted with  $d\sigma$  into the solid angle  $d\Omega$  in the direction of  $\theta$ , the Klein-Nishina obtained the equation,

$$\frac{d\sigma}{d\Omega} = r_0^2 (hv/hv')^2 \left( hv/hv' + hv'/hv - \sin \alpha \pm \sin \beta = 2 \sin \frac{1}{2}(\alpha \pm \beta) \sin^2 \theta \right) d\sigma d\Omega \dots \dots (8)$$

Here  $r_0$  is and the cross-section can be approximated as [19],

$$\sigma_c \approx \frac{\alpha^2 (hc)^2}{4\pi^2 W^2} \dots \dots (9)$$

$W$  is the centre of mass energy of the photon electron system and given by,

$$W = \sqrt{(m_e c^2)^2 + 2E_\gamma m_e c^2}$$

For pair production, the cross section is depended on  $Z$  also, the relation is following,

$$\sigma_{pp} \approx \frac{Z^3 \alpha^3}{m_e^2 c^4} \dots \dots (10)$$

So, high  $Z$  material is more likely to interact with photons and photons will interact with material and give pair production.

## 6. Results and Discussion

### 6.1 Total mass attenuation coefficient ( $\mu_m$ )

The mass attenuation coefficient computed using Eq. (1) and the XCOM values for the five-shielding slab across an energy range of 40 keV to 20 MeV are presented in Table 1. It can be seen that the derived values from Geant4, X-com values of mass attenuation coefficients are in fine compatibility. The variation of the values for these five materials are presented in Fig 3.

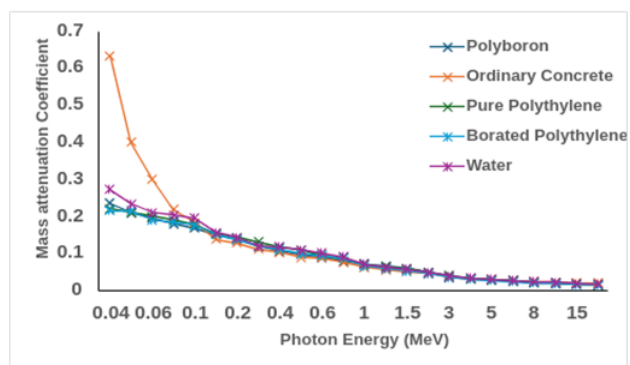


Figure 3: The mass attenuation coefficient of the shielding materials varies as a function of photon energy.

Figure 3 makes it clear that mass attenuation coefficient depends on incident gamma ray energy as well as it depends on the composition of material of the shielding materials and decreases if incident photon energy is increased. Figure 3 illustrates the relation between the mass attenuation coefficient and photon energy. Observation indicates that the highest mass attenuation coefficient over an energy range 40 keV to 0.125 MeV has ordinary concrete. From this figure, it is evident that the mass attenuation coefficient of ordinary concrete reduces with increasing photon energy. Materials which have the high atomic number are more effective for gamma-ray shielding. The highest mass attenuation coefficient is of ordinary concrete. Among the interactions of gamma ray, as photoelectric effect is predominant at low energy regions the gamma ray is attenuated easily. Borated polyethylene has the highest amount of boron by weight percentage but shows the minimum mass attenuation coefficient. The materials, ranked in order of decreasing mass attenuation coefficient within the specified energy range, are as follows:  
ordinary concrete > water > polyboron > polyethylene > borated polyethylene

From Fig.3 it shows that increase in the photon energy leads to the mass attenuation coefficient decreases and when the energy of a photon goes over 0.125 MeV, the mass attenuation coefficient of all the shielding materials possess approximately the same value over a particular energy range. As at the intermediate energy range, Compton scattering predominates and this phenomenon is observed. The mass attenuation coefficient depends on the ratio of atomic number to the atomic weight for all elements and which is around equal to  $\frac{1}{2}$  except for hydrogen and the heavy elements [15].

It signifies that at those energies where Compton scattering predominates, the mass attenuation coefficients are typically consistent across different elements, and most materials exhibit almost nearly identical gamma ray attenuation properties when evaluated on a mass basis. Pair production starts to be dominant for all the sample, when the photon energy tends to cross 1.02 MeV and that's why all the present sample materials possess around the same mass attenuation coefficient over 1.02 MeV.

### 6.2 Linear attenuation coefficient ( $\mu$ )

Fig. 4 demonstrates dependency on energy of the linear attenuation coefficient. The nature of the curve for each material remains approximately the same. By calculating the linear attenuation coefficient of each compound which is by multiplying density with the mass attenuation coefficient. From this figure, it is apparent that the highest linear attenuation coefficient across the entire photon energy range is for ordinary concrete which is due to its high density and the availability of high atomic numbered elements.

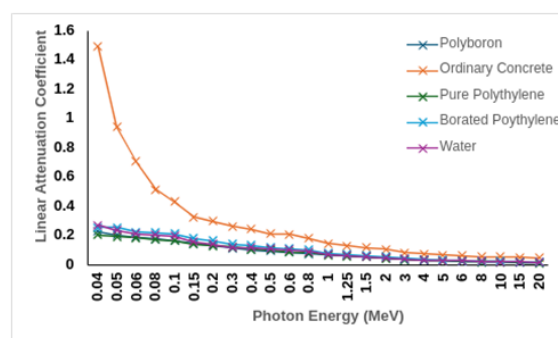


Figure 4: Linear attenuation coefficient of the

shielding materials as a function of photon energy

### 6.3 Relaxation length ( $\lambda$ )

The relaxation length is computed from by Eq. (5) of the five sample materials changing energy of photon from 40 keV to 20 MeV and its dependency on photon energy has been presented in Fig. 5. The shielding effectiveness improves as the relaxation length decreases. Mathematically this parameter is same as the inverse of linear attenuation coefficient. The ordinary concrete has the smallest relaxation length so that it is more efficient than other materials relatively in shielding.

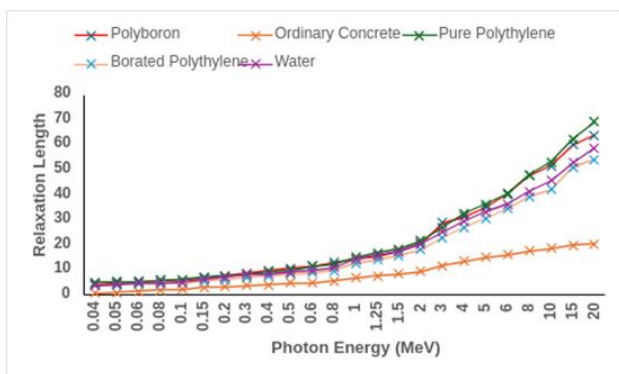


Figure 5: Relaxation Length of the shielding materials as a function of Photon energy

### 6.4 The Half Value Layer (HVL) and Tenth Value Layer (TVL) for various common gamma sources

In Table 2, the HVL and TVL values for five sample materials have been provided for several common gamma sources. Sources like Cs-137 (0.662 MeV), Co-60 (1.1732 MeV, 1.3325 MeV), N-16 (7.12 MeV), I-131 (0.364 MeV) and Na-24 (2.75 MeV) are widely used in various purposes [7] [9]. The Half Value Layer (HVL), Tenth Value Layer (TVL) are key parameters in the design of radiation shielding. HVL and TVL is the required thickness of a shield to decrease the dose/intensity level of radiation to half and one tenth of its initial value respectively. This study can help in selecting the suitable shielding materials for these gamma sources. Study mentioned in this paper demonstrates that

ordinary concrete provides the best shielding properties, as it has the smallest TVL and HVL. So, ordinary concrete will be the most suitable shielding for these gamma sources. The value of HVL and TVL deviates from standard literature value. The root mean square differences between the literature and simulated value has been calculated. Assuming the XCOM values as true values, the RMS increased with an increasing difference between the XCOM and GEANT4 values. The rms values for HVL and TVL are reported in Table 3 and Table 4 respectively. RMS difference formula is stated below,

$$X_{rms} = \sqrt{\frac{x_1^2 + x_2^2 + x_3^2 + \dots + x_n^2}{n}} \dots \dots (11)$$

Here,  $X_i = X_{XCOM} - X_{GEANT4}$

The HVL and TVL values for each source and five different samples have been illustrated in figure 6,7,8,9 and 10. A typical curve on radiation attenuation factor at gamma-ray energy of 511 keV for different shielding materials is shown in Figure 11. The graphs illustrate the exponential decline behavior that is consistent with equation (1). Every material exhibits the anticipated exponential drop in gamma intensity as penetration depth increases. Regarding 511 keV photons (such as those used in PET imaging and annihilation photons):

Even 10 cm of concrete only attenuates about 82%, thus thin shields are insufficient. In practice, multi-layered shielding—such as thick + hydrogenous layers—is frequently favored.

Plotting  $I/I_0$  vs. thickness  $x$  results in an exponentially decaying curve that is shallower for materials like water or pure PE and steeper for high- $\mu$  materials like concrete or poly-boron. Shielding surrounding reactors, spent fuel, and transport containers is designed with the use of attenuation calculations.

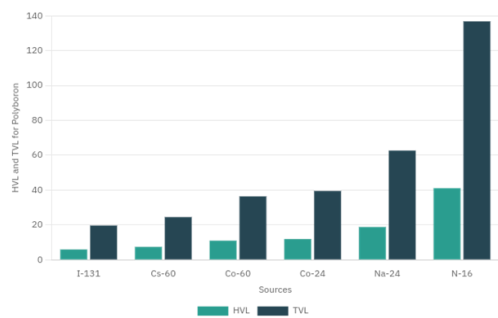


Figure 6: HVL and TVL value for different sources for Polyboron

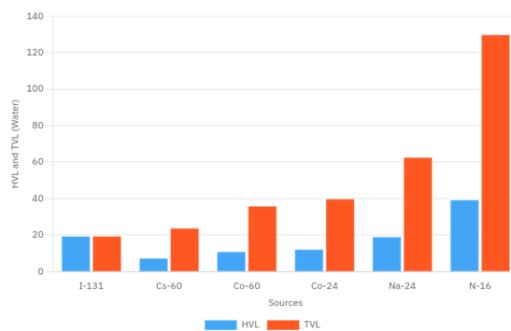


Figure 10: HVL and TVL values for different sources for Water

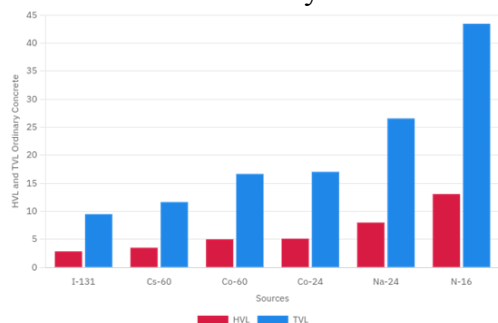


Figure 7: HVL and TVL Value for different sources for Ordinary Concrete

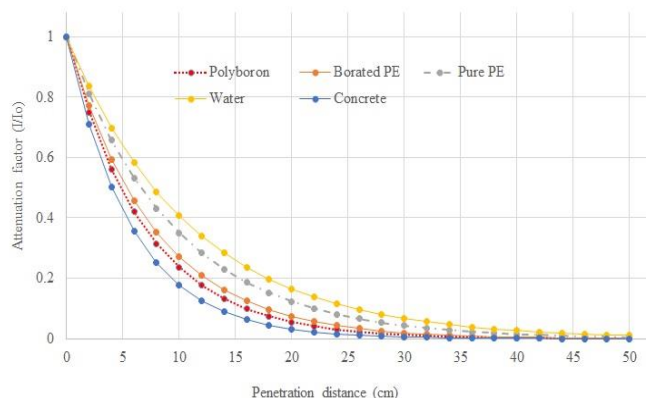


Figure 11: Attenuation factor vs. penetration distance for 511 keV for different materials.

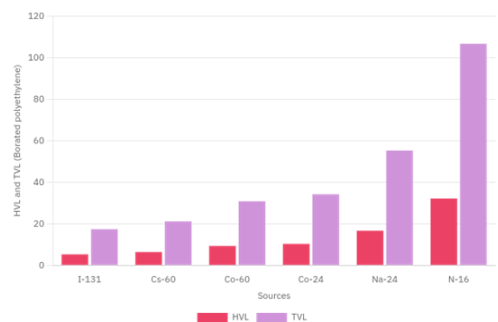


Figure 8: HVL and TVL Value for different sources for Borated Polyethylene

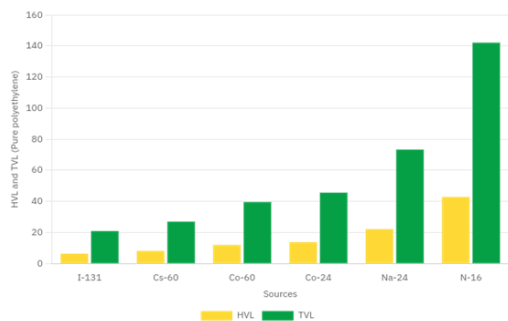


Figure 9: HVL and TVL Value for different sources for Pure Polyethylene

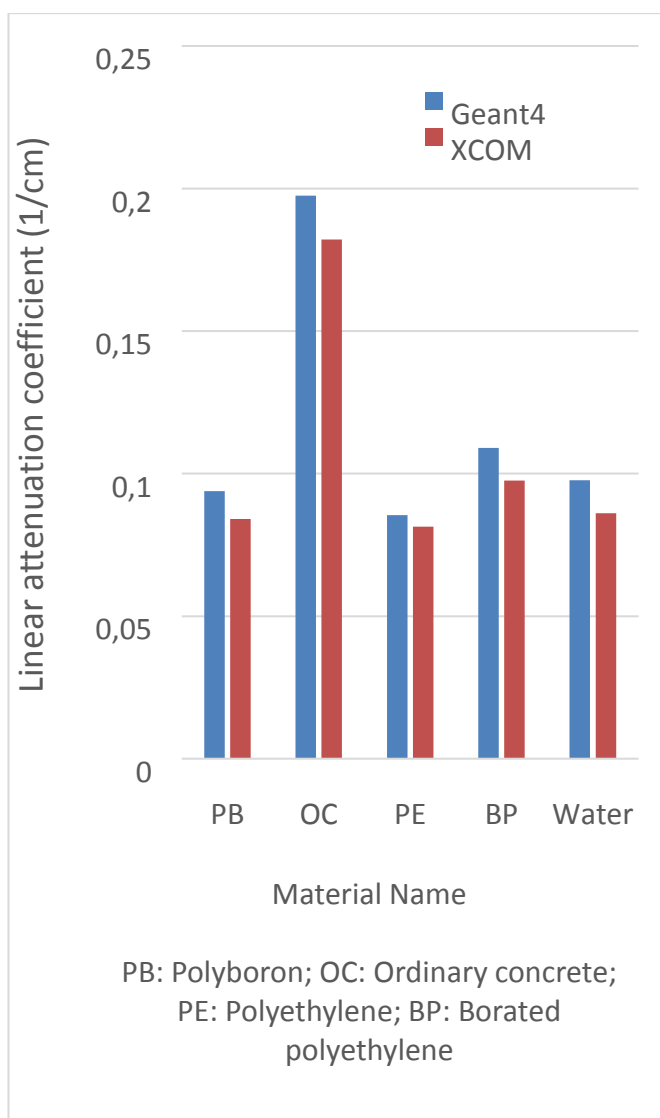


Figure 12: Linear attenuation coefficient at 662 keV for different shielding materials.

For comparison purposes, the linear attenuation coefficient ( $\mu$ ) for different shielding materials at 662 keV is shown in Fig. 12 using two software. From Fig. 12, one can easily calculate the linear attenuation coefficient and can be used for any shielding design using Cs-137 source (662 keV). The results are reasonably good agreement between Geant4 and XCOM.

### 6.5 Interpretation of the Material by Material

Shielding materials are essential for preventing ionizing radiation, particularly gamma and neutron radiation, from harming people, property, and the environment. The materials we studied—Polyboron, Borated Polyethylene, Pure

Polyethylene, Water, and Ordinary Concrete—have special interaction properties that make them essential in a variety of industrial, medical, and nuclear applications. Table 5 provides an overview of the materials' interactions and significance. Neutron and gamma-ray mixed fields are produced in the majority of radiation environments, such as reactors and cyclotrons. These are some of the most effective materials attenuating both. Strict national and international standards (such as those set by the IAEA, BAEC, and BAERA) must be followed when shielding. Regulatory frameworks have validated and approved these materials. Table 5 provides an overview of the materials' interactions and significance. Based on the information, the end users can select the materials for primary purposes.

Table 5: Primary use and importance of different shielding materials.

Material	Primary Use	Importance
Ordinary Concrete	Reactor walls, bunkers, hot cells	Inexpensive, dense, and effective against gamma rays due to calcium, silicon, and iron content. Neutron attenuation depends on hydration level and composition. Easy to shape in bulk.
Polyboron	Neutron shielding in nuclear reactors and containers	Combines high hydrogen content (for moderating fast neutrons) with boron (excellent thermal neutron absorber). Offers good dual protection in compact form.
Borated Polyethylene	Reactor shielding, spent fuel storage, PET labs	Polyethylene slows down fast neutrons, and boron captures them. Used extensively where neutron-rich fields exist. Easy to machine and non-toxic.
Pure Polyethylene	Neutron moderation	Rich in hydrogen atoms, it is excellent at slowing fast neutrons (but not absorbing them). Often used as the first layer before a boron-rich material.
Water	Primary coolant and biological shield in reactors	Natural hydrogen content makes it a cost-effective moderator and shield for both gamma and neutron radiation. Also used as a temporary or emergency shield.

## 7 Conclusion

The study concludes that the density, chemical composition, and element concentration in a shielding material all influence its shielding effectiveness. It is established that all the nuclear related parameters related to it have to be studied thoroughly. In this research, the gamma radiation attenuation parameters have been studied for locally developed shielding materials. Over a certain photon energy range (40 keV to 20 MeV), it is identified that ordinary concrete possesses better gamma-ray attenuation characteristics among the sample materials. Considering factors such as local availability, cost and ease of

fabrication, ordinary concrete is a viable option for use as biological shielding against gamma rays. This study can further use for improving shielding condition of polyboron. The simulated results of this study can serve as preliminary data, with further experimental work planned for future investigations. By calculating the nuclear parameters GEANT4 toolkit has been validated with some marginal errors. GEANT4 can be recommended for studying the changes of attenuation properties of other sample materials to develop a simplified virtual model for gamma and neutron transport calculations. In situations with neutron-gamma mixed radiation, polyboron and borated PE can be customized in terms of boron content, form, or embedding in multilayered systems.

## 8 Future Direction

Material selection is based on application, weight, cost, and necessary attenuation. These materials are engineered solutions intended to maximize safety, utility, and cost-effectiveness in radiation situations; they are more than merely barriers. As radiation technologies advance, it is crucial that they be continuously studied, optimized, and combined. Complex engineering issues can be solved numerically with finite element analysis (FEA). FEA [12] [13] is used to model and examine how structures and materials attenuate ionizing radiation in the context of radiation shielding. This aids in forecasting the efficacy of shielding designs and materials prior to the construction of physical prototypes. The primary goal of this study is to use solely gamma-ray attenuation using GENT4 and XCOM; employing FEA is outside the purview of this investigation. Using COMSOLS or ANSYS software, FEA will be used in the future for radiation attenuation studies. Additionally, MCNP, SuperMC and Machine Learning (ML) are intended to be used for validation in the neutron and gamma-ray mixed fields. Further

study's findings can be used for biological shielding, nuclear reactor shielding, containment buildings, nuclear spent fuel transportation and storage casks in Rooppur nuclear power plant and other radiation facilities in the context of Bangladesh.

## Acknowledgement

The authors show their gratitude to the Department of Nuclear Science and Engineering at the Military Institute of Science and Technology for providing all the essential facilities.

Table 1: The Geant4 and X-Com values (including coherent scattering) of mass attenuation coefficients ( $\text{cm}^2/\text{g}$ ) for sample shielding materials

Photon Energy (MeV)	Polyboron		Ordinary concrete		Pure Polyethylene		Borated Polyethylene		Water	
	Geant4	XCOM	Geant4	XCOM	Geant4	XCOM	Geant4	XCOM	Geant4	XCOM
0.04	0.236	0.235	0.6338	0.613	0.221	0.2275	0.2164	0.2129	0.2729	0.2683
0.05	0.211	0.2104	0.4012	0.3948	0.21	0.2084	0.215	0.1948	0.2345	0.2269
0.06	0.1959	0.1967	0.30034	0.2959	0.201	0.197	0.1901	0.184	0.2113	0.2059
0.08	0.1811	0.1802	0.2184	0.2126	0.1898	0.1823	0.1848	0.1701	0.2039	0.1837
0.1	0.1695	0.1693	0.1843	0.1784	0.1794	0.1719	0.1771	0.1604	0.1951	0.1707
0.15	0.1512	0.1506	0.1393	0.1434	0.1528	0.1534	0.1512	0.1431	0.1567	0.1505
0.2	0.1373	0.1375	0.128	0.127	0.1428	0.1402	0.1384	0.1307	0.1427	0.137
0.3	0.1193	0.1193	0.1123	0.1082	0.132	0.1217	0.1201	0.1134	0.1201	0.1186
0.4	0.1064	0.1068	0.1032	0.09628	0.1164	0.1089	0.1123	0.1016	0.1185	0.1061
0.5	0.0974	0.09748	0.0901	0.08768	0.1101	0.09947	0.1006	0.09274	0.1099	0.09687
0.6	0.0902	0.09014	0.0886	0.08098	0.0953	0.09198	0.0946	0.08576	0.1023	0.08956
0.8	0.07915	0.07915	0.0769	0.07103	0.0885	0.08078	0.0875	0.07531	0.0917	0.07866

1	0.07178	0.07	0.0621	0.0635	0.07184	0.07262	0.06643	0.06772	0.0706	0.07072
1.25	0.06596	0.06	0.0559	0.05678	0.06421	0.06495	0.06	0.06056	0.0631	0.06323
1.5	0.05915	0.06	0.05078	0.05171	0.0589	0.0591	0.053	0.0551	0.0574	0.05754
2	0.0496	0.05	0.04588	0.0446	0.0501	0.05064	0.0467	0.04723	0.0493	0.04942
3	0.03576	0.04	0.03627	0.03636	0.0403	0.04045	0.0367	0.03774	0.0396	0.03969
4	0.03285	0.03	0.03165	0.03174	0.0332	0.03444	0.0312	0.03215	0.0339	0.03403
5	0.02949	0.03002	0.0285	0.02881	0.03	0.03045	0.02744	0.02845	0.0302	0.03031
6	0.02538	0.02728	0.0267	0.02683	0.0269	0.0276	0.02434	0.02581	0.0276	0.0277
8	0.02153	0.02366	0.02429	0.02438	0.0227	0.02383	0.02134	0.02232	0.0242	0.02429
10	0.01995	0.02139	0.023	0.023	0.02045	0.02145	0.0199	0.02012	0.0219	0.02219
15	0.01718	0.01831	0.0214	0.02143	0.01745	0.01819	0.01645	0.01712	0.0189	0.01941
20	0.01611	0.01681	0.0209	0.02095	0.01571	0.01658	0.0155	0.01565	0.017	0.01813

Table 2: The calculation of the Half Value Layer (HVL) and the Tenth Value Layer (TVL) for various gamma sources across different sample materials

Photon Energy (MeV)	Source Identity	Polyboron		Ordinary concrete		Pure Polyethylene		Borated Polyethylene		Water	
		HVL	TVL	HVL	TVL	HVL	TVL	HVL	TVL	HVL	TVL
0.364	I-131	5.919	19.66	2.8571	9.4912	6.2841	20.8756	5.211	17.31	19.17	19.175
0.662	Cs-60	7.381	24.5	3.509	11.658	8.11641	26.9623	6.353	21.10	7.094	23.567
1.1732	Co-60	10.95	36.38	5.0155	16.661	11.90	39.56	9.266	30.78	10.72	35.64
1.3325	Co-24	11.88	39.48	5.1306	17.043	13.725	45.5957	10.28	34.16	11.90	39.542
2.75	Na-24	18.801	62.68	7.9987	26.558	22.074	73.33	16.622	55.211	18.7844	62.401
7.12	N-16	41.111	136.8	13.078	43.445	42.785	142.15	32.099	106.604	39.073	129.653

Table 3: RMS Differences between XCOM and GEANT4 measured HVL values

Polyboron			Ordinary Concrete			Polyethylene			Borated Polyethylene			Water		
XCOM	GEANT4	RMS	XCOM	GEANT4	RMS	XCOM	GEANT4	RMS	XCOM	GEANT4	RMS	XCOM	GEANT4	RMS
6.41	5.919	5.319	2.95	2.8571	0.64	6.64	6.2841	5.77	5.53	5.211	3.21	6.26	6.35	6.27
8.23	7.381		3.8	3.509		8.51	8.11641		7.1	6.353		8.04	7.094	
10.82	10.95		5.01	5.0155		11.19	11.90		9.33	9.266		10.58	10.72	
11.56	11.88		5.35	5.1306		11.95	13.725		9.97	10.28		16.45	11.90	
16.91	18.801		7.68	7.9987		17.52	22.07		14.6	16.622		26.87	18.7844	
28.26	41.111		11.58	13.078		29.55	42.785		24.54	32.099		26.87	39.073	

Table 4: RMS Differences between XCOM and GEANT4 measured TVL values

Polyboron			Ordinary Concrete			Polyethylene			Borated Polyethylene			Water		
XCOM	GEANT4	RMS	XCOM	GEANT4	RMS	XCOM	GEANT4	RMS	XCOM	GEANT4	RMS	XCOM	GEANT4	RMS
21.32	19.66	17.76	9.79	9.4912	2.127	22.05	20.8756	19.16	18.39	17.31	10.646	20.81	19.175	16.852
27.35	24.5		12.64	11.65		28.28	26.962		23.58	21.10		26.72	23.567	
35.96	36.38		16.65	16.661		37.19	39.56		31.01	30.78		35.14	35.64	
38.41	39.48		17.78	17.043		39.72	45.595		33.12	34.16		37.54	39.542	
56.2	62.68		25.51	26.55		58.22	73.33		48.51	55.211		54.68	62.401	
93.92	136.8		38.5	43.445		98.2	142.15		81.57	106.604		89.31	129.653	

### References

- [1] Cember, H. and Johnson, T. E. (2009). Introduction to Health Physics, 4<sup>th</sup> Edition, The McGraw-Hill Companies, Inc.
- [2] Biswas, R., Sahadath, H., Mollah, A. S., and Huq, M. F. (2015). Calculation of gamma-ray attenuation parameters for locally developed shielding material: Polyboron. *Journal of Radiation Research and Applied Sciences*, 9(1), 26–34.  
<https://doi.org/10.1016/j.jrras.2015.08.005>
- [3] Akkurt, I., Akyıldırım, H., Mavi, B., Kilincarslan, S., and Basyigit, C. (2010). Photon attenuation coefficients of concrete includes barite in different rate. *Annals of Nuclear Energy*, 37(7), 910–914.  
<https://doi.org/10.1016/j.anucene.2010.04.001>
- [4] Iqbal, S. M., Rahman, A., Fakarudin, M., Nor Paiza, M. H., and Ismail, M. (2011). Mass attenuation coefficients, effective atomic and electron numbers of stainless steel and carbon steels with different energies. *Jurnal Sains Nuklear Malaysia*, 23(2), 19-25.
- [5] El-Khayatt, A. M. (2010). Radiation shielding of concretes containing different lime/silica ratios. *Annals of Nuclear Energy*, 37, 991-995.
- [6] El-Khayatt, A. M., and Akkurt, I. (2013). Photon interaction, energy absorption and neutron removal cross section of concrete including marble. *Annals of Nuclear Energy*, 60, 8-14.
- [7] Rasoul Mehrnejad, Abdulhalik Karabulut, Turgay Korkut, and Bunyamin Aygu, Improving Neutron Shielding Capacities of Galena and Barite Hybrid Fiber Heavyweight Aggregate Concrete for Nuclear Reactor, *International Journal on Applied Physics and Engineering*, Volume 2, 128-136, 2023 DOI: 10.37394/232030.2023.2.12
- [8] Chaobin Chen, Qi Yang, Bin Wu, Yuncheng Han, Jing Song and FDS Team (2017). Validation of Shielding Analysis Capability of SuperMC with SINBAD, EPJ Web of Conferences 153, 02009 (2017). DOI: 10.1051/epjconf/20171530.
- [9] Huda, M. Q., Bhuiyan, S. I., Ahmed, F. U., Mollah, A. S., and Mondal, M. A. W. (1998). MCNP4B verification on experimental studies of neutron shielding properties of ilmenite-magnetite concrete and polyboron using a <sup>252</sup>Cf source. In 1998 ANS Radiation Protection and Shielding Division Tropical Conference, Technologies for the New Century, April 19-23 (Vol. 2, pp. 344-349).
- [10] Stanislav Kovář, Jan Valouch, Hana Urbančoková, Milan Adámek and Václav Mach, Simulation of Shielding Effectiveness of Materials using CST Studio, *WSEAS Transactions on Communications*, Volume 16, 2017, 131-136.
- [11] Igor Ogorevc, Yasihoro Shimotsuura, Irma Ogorevc, and Slavisa Stanisic, Natural Protection from Nuclear Accidents in the Environment Radiation Protection for Everyone, *WSEAS Transactions on Biology and Biomedicine*, Volume 22, 118-122, 2025 DOI: 10.37394/23208.2025.22.14
- [12] Sarah David Müzel, Eduardo Pires Bonhin, Nara Miranda Guimarães and Erick Siqueira Guidi, Application of the Finite Element Method in the Analysis of Composite Materials: A Review, *Polymers* 2020, 12, 818; doi:10.3390/polym12040818
- [13] Boahen, J. K., Mohamed, S. A. E., Khalil, A. S. G., and Hassan, M. A. (2022). Finite Element Formulation and Simulation of Gamma Ray Attenuation of Single and Multilayer Materials Using Lead, Tungsten and EPDM. *Materials Science Forum*, 1069, 87-94.

[14] Elmahroug, Y., Tellili, B., and Souga, C. (2013). Calculation of gamma and neutron shielding parameters for some materials polyethylene-based. *International Journal of Physics and Research*, 3, 33-40.

[15] Hubbell, J. H., and Seltzer, S. M. (1995). Tables of X-ray mass attenuation coefficients and mass energy-absorption coefficients 1 keV to 20 MeV for elements  $Z=1$  to 92 and 48 additional substances of dosimetric interest. NISTIR-5632. Gaithersburg: National Institute of Standards and Technology.

[16] Geant4 - A Simulation Toolkit, S. Agostinelli et al., *Nucl. Instrum. Meth. A* 506 (2003) 250-303

[17] Pratt, R. H. (1960). Atomic photoelectric effect at high energies. *Physical Review*, 117(4), 1017–1028.

<https://doi.org/10.1103/physrev.117.1017>

[18] Gavrila, M. (1959). RelativisticK-Shell photoeffect. *Physical Review*, 113(2), 514–526.

<https://doi.org/10.1103/physrev.113.514>

[19] Williams, W. S. C. (1990). *Nuclear and particle physics*. Oxford University Press, p. 250-251.

[20] Jobe, J. D., and St John, R. M. (1967). Absolute measurements of the  $^{21}\text{P}$  and  $^{23}\text{P}$  Electron excitation *Physical Review*, 164(1), 117–121.

<https://doi.org/10.1103/physrev.164.117>